

A search for radio emission from Galactic supersoft X-ray sources

R. N. Ogle¹★ S. Chaty,² M. Crocker,³ S. P. S. Eyres,⁴ M. A. Kenworthy,⁵
A. M. S. Richards,³ L. F. Rodríguez⁶ and A. M. Stirling⁴

¹*Department of Physics, Keele University, Staffordshire ST5 5BG*

²*Department of Physics and Astronomy, The Open University, Walton Hall, Milton Keynes, Buckinghamshire MK7 6AA*

³*University of Manchester, Jodrell Bank Observatory, Macclesfield, Cheshire SK11 9DL*

⁴*CFA, University of Central Lancashire, Preston PR1 2HE*

⁵*Steward Observatory, 933 North Cherry Avenue, Tucson, AZ 85721, USA*

⁶*Instituto de Astronomía, UNAM, Campus Morelia, Apdo. Postal 3-72, Morelia, Michoacán 58089, Mexico*

Accepted 2001 November 6. Received 2001 November 6; in original form 2001 July 23

ABSTRACT

We have made a deep search for radio emission from all the northern hemisphere supersoft X-ray sources using the Very Large Array (VLA) and multi-element radio-linked interferometer network (MERLIN) telescopes, at 5 and 8.4 GHz. Three previously undetected sources, T Pyx, V1974 Cygni and RX J0019.8+2156, were imaged in quiescence using the VLA in order to search for any persistent emission. No radio emission was detected in any of the VLA fields down to a typical 1σ rms noise of $20 \mu\text{Jy beam}^{-1}$, however, 17 new point sources were detected in the fields with 5-GHz fluxes between 100 and 1500 μJy , giving an average 100- μJy source density of $\sim 200 \text{ deg}^{-2}$, comparable to what was found in the MERLIN *Hubble Deep Field* survey. The persistent source AG Draconis was observed by MERLIN to provide a confirmation of previous VLA observations and to investigate the source at a higher resolution. The core is resolved at the milliarcsec scale into two components that have a combined flux of $\sim 1 \text{ mJy}$. It is possible that we are detecting nebulosity, which is becoming resolved out by the higher MERLIN resolution. We have investigated possible causes of radio emission from a wind environment, both directly from the secondary star, and also consequently, of the high X-ray luminosity from the white dwarf. There is an order of magnitude discrepancy between observed and modelled values that can be explained by the uncertainty in fundamental quantities within these systems.

Key words: binaries: general – novae, cataclysmic variables – white dwarfs – radio continuum: stars – X-rays: stars.

1 INTRODUCTION

Supersoft sources are a separate class of X-ray objects. The most popular explanation of these sources is a white dwarf and subgiant companion with a high accretion rate, 100–1000 times greater than in cataclysmic variables (van den Heuvel et al. 1992). The large accretion rate creates steady hydrogen burning on the white dwarf surface causing X-ray emission.

Supersoft sources are difficult to detect in the Galaxy as the high column density in the Galactic plane absorbs most of the soft X-ray radiation. Consequently, there have been many more detections at high galactic latitudes such as in the Large Magellanic Cloud (LMC), Small Magellanic Cloud (SMC) and M31. As of 1999 (Greiner 2000), there were 57 supersoft sources: 10 in the Galaxy, four in the SMC, eight in the LMC and 34 in M31 and one in NGC

55. Consequently, even though sources in the LMC and SMC are further away, they have been studied in greater detail because of their larger numbers. For example, in 1997 Fender, Southwell & Tzioumis (1998) searched for radio emission from non-Galactic supersoft sources despite them being prohibitively further away than their Galactic counterparts.

Of the persistent supersoft sources, three have been reported to have outflows, detected by emission lines in their optical and infrared spectra. What is the make-up of these sources, and are they the link between the low-velocity jets seen in star-forming systems and the superluminal jets seen in microquasars?

1.1 Sources with outflow

Three supersoft sources have been observed with weak Doppler-shifted optical emission lines. The first object to be detected was RX J0513.9–6951, an LMC object that was discovered during an

★E-mail: rno@astro.keele.ac.uk

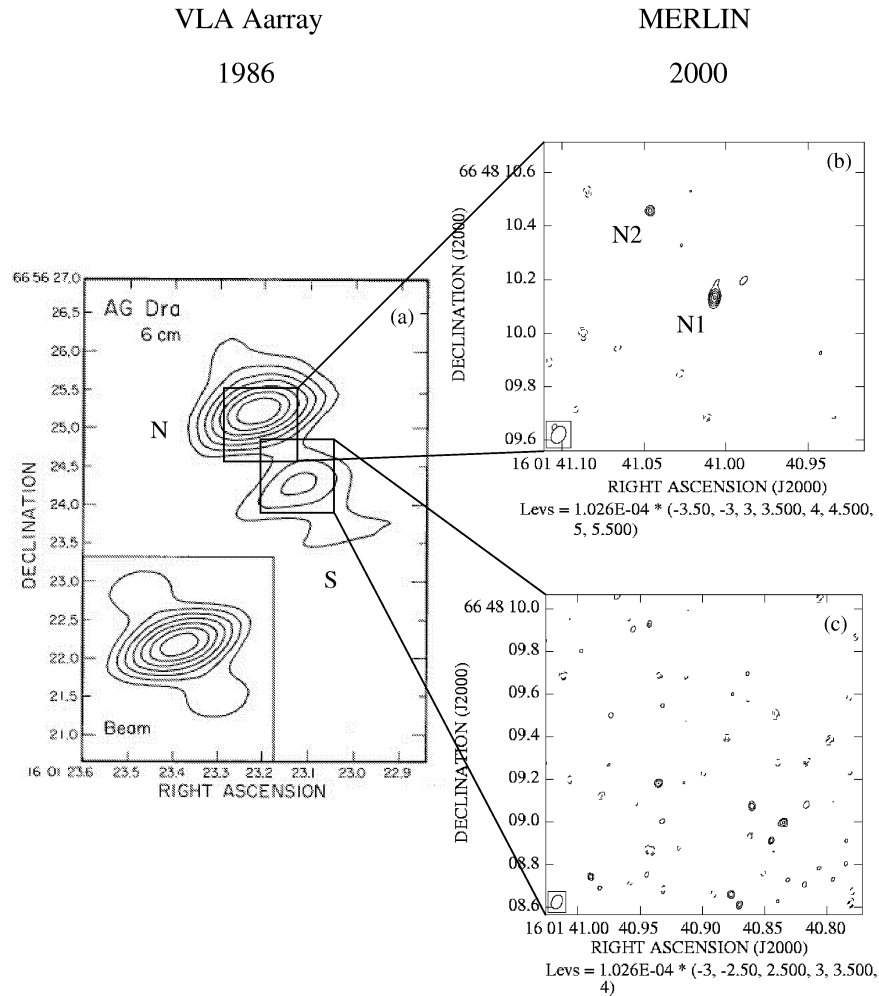


Figure 1. (a) Previous VLA observations of AG Dra. (Torbett & Campbell 1987). (b) Higher-resolution MERLIN observations at 4.994 GHz. The core is clearly detected and resolved into two components at the $48.9 \times 68.5 \text{ mas}^2$ resolution (as shown by the beam in the lower left-hand corner). Any extension in component N1 is probably caused by noise in the image. Fluxes of components N1 and N2 are 570 and 420 μJy , respectively. It is possible that we are resolving out any extended nebulosity around the core in the MERLIN image. (c) MERLIN observations of the southern VLA component with lower contours to bring out the noise in the image. There are no clear detections of emission.

outburst in 1990 (Schaeidt, Hasinger & Trümper 1993), and identified optically by Pakull et al. (1993) and Cowley et al. (1993). This source has persistent optical emission with dips in the light curve every 100–200 d (Southwell et al. 1996). The evidence for jets in this source comes from strong He II, H β and H α lines with Doppler-shifted components at $\pm 4000 \text{ km s}^{-1}$ (Southwell et al. 1996). These lines are still observed during an optical dip, but with a reduced equivalent width, implying a reduction in the accretion rate.

The second supersoft jet source to be detected was RX J0019.8+2156 (Beuermann et al. 1995), a Galactic object at 2 kpc consisting of a 1- M_{\odot} white dwarf (WD) and a 1.5- M_{\odot} donor star (Becker et al. 1998). The optical spectrum shows strong He II emission and P Cygni absorption in the Balmer lines. This source displays slower red- and blueshifted lines with velocities of $\pm 815 \text{ km s}^{-1}$, but these lines have a high FWHM of 400 km s^{-1} (Tomov et al. 1998). Quaintrell & Fender (1998) have also found these features in infrared spectra. Becker et al. (1998) conclude that the jets in this system come from an inclined cone of material blown off from an accretion disc.

The third, and last, supersoft source to be discovered with an outflow is the Galactic source RX J0925.7–4758. This was observed by Motch (1998) over two nights in 1997. Spectra showed prominent H α blue- and redshifted lines with a velocity of 5800 km s^{-1} . Motch (1998) modelled the emission from a cone with a large opening angle, at low inclination, similar to RX J0019+2156.

The only radio detection of a supersoft source was that of the symbiotic star AG Draconis (Torbett & Campbell 1987; Seaquist et al. 1993). Observations with the VLA showed two unresolved components separated by ≈ 1 arcsec, at fluxes of 200 and 400 μJy , shown in Fig. 1(a). These authors conclude that the emission is from optically thick thermal free–free emission, based on the majority of symbiotic systems. However, we cannot rule out optically thick emission in this paper.

2 OBSERVATIONS

Of the 10 Galactic supersoft sources, four were observed by the VLA. These are RX J0019.8+2156, T Pyx, AG Draconis and

V1974 Cygni. Three of these sources were observed with the VLA with the exception of AG Dra, which was observed using MERLIN for the purpose of resolving any detail.

As we were concerned primarily with initial detections of point sources, a standard continuum setup was used for both the VLA and MERLIN observations. For the VLA we used a 100-MHz bandwidth split into two channels, and for MERLIN we used a 15-MHz bandwidth split into 15 channels. Individual channels were retained in order to reduce the amount of bandwidth smearing of sources offset from the phase centre.

2.1 T Pyxis

T Pyx is a recurrent nova first discovered by Leavitt (1914) at a distance of 1.5 kpc (Shara et al. 1997; Margon & Deutsch 1998). An arcsec-size optical nebula around the source, which shows a large amount of clumpy material on subarcsec scales, was detected from this object (Williams 1982; Duerbeck & Sitter 1987). This clumpy material would provide a rich medium for interaction with an outflow, such as the 1100–1400 km s⁻¹ jets reported by Shabbaz et al. (1997) [however, this outflow probably originates in the surrounding nebular, and not in jets, see O’Brien & Cohen (1998) and Margon & Deutsch (1998)].

Observations were taken using the VLA in CnB configuration on 2000 March 3, 0415–0615 UT at 8.4 GHz and in D configuration on 2000 September 26 and 28, 1600–1710 and 1400–1630 UT, respectively. Data were calibrated using the standard flux calibrator 3C 147, and phase calibrator PKS J0921–2618. No emission was observed from either the source, or any of the seven surrounding sources from the SIMBAD data base. We can put a 1 σ rms upper limit of 22 μ Jy beam⁻¹ at 4.8 GHz, and 19 μ Jy beam⁻¹ at 8.4 GHz.

An observing log, together with beam sizes, rms noise and source details for all sources is given in Table 1.

2.2 V1974 Cygni (\equiv Nova Cygni 1992)

V1974 Cygni was studied extensively at all wavelengths following an outburst in 1992. Complementary VLA and MERLIN images show that the source initially flared then decayed, as a shell from the outburst expanded (Hjellming 1992; Eyres, Davis & Bode 1996). They concluded that the emission from the nova was thermal and initially optically thick, then gradually became optically thin. This is expected from an expanding shell of material.

This source was observed by the VLA in CnB configuration on 2000 March 9 and 10 at 1500–1600 and 1330–1430 UT, respectively, at 8.4 GHz and in DnC configuration on 2000 June 27 at 0800–0945 UT at 4.8 GHz. Data were calibrated using the standard flux calibrator 3C 286 and phase-referenced using Ohio W 538. No emission was detected from Nova Cygni 1992. We can put a 1 σ rms upper limit to any emission of 24.6 μ Jy beam⁻¹ at 4.8 GHz, and 19.8 μ Jy beam⁻¹ at 8.4 GHz.

2.3 RX J0019.8+2156 (\equiv QR Andromedae)

RX J0019.8+2156 was observed using the VLA in CnB configuration on 2000 March 11 at 1810–2050 UT at 8.4 GHz and in DnC configuration on 2000 June 27 at 1300–1530 UT at 4.8 GHz. The flux calibrator used was 3C 48 and the data were phase-referenced using PKS J0010+1724. No emission was detected from RX J0019.8+2156. We can therefore put a 1 σ rms

Table 1. Observation log and source details. Please note that the MERLIN observations are only at 5 GHz and the two fluxes presented are for two components in the image.

T Pyx		
Band	4.8 GHz (C)	8.4 GHz (X)
Telescope	VLA D	VLA CnB
Date (2000)	Sep 26 1600–1710 Sep 28 1400–1630	Mar 03 0415–0615
MJD	51 813 51 815	51 606
Flux cal	3C 147	
Phase cal	PKS J0921–2618	
1 σ rms	22 μ Jy beam ⁻¹	19 μ Jy beam ⁻¹
Beam size	28 ^o 9 \times 10 ^o 40	2 ^o 12 \times 2 ^o 04
Beam angle	–3 ^o 98	47 ^o 6
V1974 Cygni (\equiv Nova Cygni 1992)		
Band	4.8 GHz (C)	8.4 GHz (X)
Telescope	VLA DnC	VLA CnB
Date (2000)	Jun 27 0800–0945	Mar 09 1500–1600 Mar 10 1330–1430
MJD	51 722	51 612 51 613
Flux cal	3C 286	
Phase cal	Ohio W 538	
1 σ rms	24.6 μ Jy beam ⁻¹	19.8 μ Jy beam ⁻¹
Beam size	13 ^o 8 \times 8 ^o 03	2 ^o 12 \times 0 ^o 92
Beam angle	88 ^o 9	–79 ^o 83
RX J0019.8+2156 (\equiv QR And)		
Band	4.8 GHz (C)	8.4 GHz (X)
Telescope	VLA DnC	VLA CnB
Date (2000)	Jun 27 1300–1530	Mar 11 1810–2050
MJD	51 722	51 614
Flux cal	3C 48	
Phase cal	PKS J0010+1724	
1 σ rms	22.7 μ Jy beam ⁻¹	19.8 μ Jy beam ⁻¹
Beam size	13 ^o 3 \times 8 ^o 12	2 ^o 19 \times 0 ^o 95
Beam angle	76 ^o 6	–88 ^o 68
AG Dra		
Band	5.0 GHz (C)	
Telescope	MERLIN	
Date (2000)	Mar 18 1010–1130 Mar 25 0630–2140 Mar 26 0510–2250	
MJD	51 621 51 628 51 629	
Flux cal	3C 286 and OQ 208	
Phase cal	7C 1603+6954	
Peak fluxes	570 μ Jy	420 μ Jy
α_{J2000}	16 ^h 01 ^m 41 ^s .007	16 ^h 01 ^m 41 ^s .046
δ_{J2000}	66 ^o 48' 10".13	66 ^o 48' 10".46
1 σ rms	103 μ Jy beam ⁻¹	
Beam size	48.9 \times 68.5 mas	
Beam angle	–27 ^o 9	

upper limit to any emission of 22.7 μ Jy beam⁻¹ at 4.8 GHz, and 19.8 μ Jy beam⁻¹ at 8.4 GHz.

2.4 AG Draconis

To confirm the previous VLA detection, shown in Fig. 1(a), we observed AG Dra on 2000 March 18, 25 and 26 at 1010–1130,

0630–2140 and 0510–2250 UT, respectively, with MERLIN. Owing to the superior resolving power of MERLIN over the VLA we intended to resolve the two unresolved components detected previously, and obtain some information concerning the source's structure. The MERLIN image has a beam size of $48.9 \times 68.5 \text{ mas}^2$ at an angle of -27.9° , and a 1σ rms noise of $103 \mu\text{Jy beam}^{-1}$ at 4.994 GHz.

The core component is clearly detected in the MERLIN image and is resolved into two point sources at $\alpha_{J2000} = 16^{\text{h}} 01^{\text{m}} 41^{\text{s}}.007$, $\delta_{J2000} = +66^\circ 48' 10''.13$ with a flux of $570 \mu\text{Jy}$ (designated as N1 in Fig. 1b), and $\alpha_{J2000} = 16^{\text{h}} 01^{\text{m}} 41^{\text{s}}.046$, $\delta_{J2000} = +66^\circ 48' 10''.46$ and a flux of $420 \mu\text{Jy}$ (designated as N2). These fluxes imply a lower limit of $\sim 8000 \text{ K}$ for the brightness temperature, consistent with the interpretation of the emission being optically thick free-free emission, however, we do not rule out optically thin emission in this paper. We note that the extension to the north of the component N1 is probably caused by noise in the image.

The southwest component in the VLA image is not so clearly defined. If the source has not increased in flux between the epochs, and is a point source then it will be indistinguishable from the noise in the MERLIN image (shown in Fig. 1c). We do observe a number of possible point sources with fluxes around $300\text{--}350 \mu\text{Jy}$, but these are ambiguous compared with the noise. We have lowered the contours compared with Fig. 1(b) to show the noise in more detail.

2.5 New objects

All three VLA fields were imaged with a diameter of 10.2 arcmin in order to check for emission from known sources, and to detect new objects in the fields. However, interferometric images all suffer from bandwidth smearing or chromatic aberration. This is particularly important when the observed bandwidth is large and a wide field is imaged. The effects of these are to smear sources in a radial direction from the phase centre, and to reduce the observed peak flux. The consequence of this effect is that the signal-to-noise ratio increases with off-axis beam angle.

For an observation taken with a bandwidth of 50 MHz at 8.3 GHz, and with a circular beam 2 arcsec in diameter, a point source will suffer a 10 per cent reduction in flux at a distance of 3 arcmin 50 arcsec from the phase centre, and a 50 per cent reduction at a distance of around 11 arcmin, this situation becomes more severe with a smaller beam (see Bridle & Schwab 1989 for details).

We have uploaded to the CDS service for Astronomical Catalogues¹ a table that lists the sources taken from the Simbad catalogue together with our limits to the radio emission from the source based on the bandwidth-smearred 5σ rms noise. While none of the known sources were detected, we observed 17 new sources with a flux greater than 5σ . An uploaded table as above lists these new sources, together with a Gaussian-fitted flux based on the image beam, and true flux owing to the bandwidth smearing in the image, (at the bands C and X given in Table 1). A spectral index is also calculated from the bandwidth smeared fluxes and follows the convention of $S \propto \nu^\alpha$.

We can therefore estimate that the density of sources with flux $>100 \mu\text{Jy}$ is $\sim 200 \text{ sources deg}^{-2}$ at 5 GHz, broadly consistent with limits from the deep radio survey by MERLIN of the *Hubble Deep Field* (Muxlow et al. 1999). The spectral indices of these sources are generally negative or consistent with a negative value, suggesting that most are non-thermal extragalactic objects,

¹ <http://cdsweb.u-strasbg.fr/cats/Cats.htm>

however, caution has to be drawn to this conclusion since data at the two frequencies are not simultaneous, and there is a difference in angular resolution between the two frequencies.

3 WIND EMISSION

In this section we describe simple analytical models for wind emission and apply them to our sample. Initially we are not interested in where the wind comes from or what it consists of, rather that a generic wind with a particular composition, being ejected at a particular rate from a source at a given distance from us, would produce radio emission. The optically thin flux from a source with these parameters can be calculated and is given by

$$S = 23.2 \left(\frac{\dot{M}}{\mu v_{\text{km s}^{-1}}} \right)^{4/3} (\nu \gamma g Z^2)^{2/3} D^{-2} \text{ Jy}, \quad (1)$$

where \dot{M} is in $M_\odot \text{ yr}^{-1}$, μ is the mean atomic weight, $v_{\text{km s}^{-1}}$ is the wind velocity in km s^{-1} , ν is in Hz, γ is the ratio of electron to ion number density, g is the Gaunt factor, Z is the ionic charge and D is the distance in kpc (Wright & Barlow 1975). The Gaunt factor here has a slight dependence on temperature and composition and if one does not consider extremely hot winds, then it can be approximated by

$$g = 9.77 + 1.27 \log_{10}(T^{3/2}/\nu Z) \quad (2)$$

(Leitherer & Robert 1991).

We can now investigate in more detail from where the wind originates, what its expected composition is and what is the expected radio emission from such a region.

3.1 Generic secondary wind

To create sustained mass transfer between the binary components either the secondary² is undergoing Roche lobe overflow, the wind is providing the accretion via Bondi–Hoyle accretion, or both. Which scenario occurs depends on the nature of the secondary, and the binary parameters.

The symbiotic system AG Dra with a $\sim 1.5\text{-}M_\odot$ K-giant, a $\sim 0.5\text{-}M_\odot$ white dwarf and a period of 544 d does not normally fill its Roche lobe (the stellar radius of the K-giant is $\sim 30 R_\odot$ and the Roche lobe size is $\sim 170 R_\odot$). Since the system must be accreting then the logical conclusion is that the secondary is on the asymptotic giant branch (AGB) and feeding the primary by a slow, dense wind. Out of the four sources considered here, this is the most likely to be feeding its environment directly by a wind. Calculating the expected flux from this wind uses a temperature, velocity, outflow and distance of $T = 15\,000 \text{ K}$, $v = 30 \text{ km s}^{-1}$, $\dot{M} = 1.2\text{--}1.7 \times 10^{-8} M_\odot \text{ yr}^{-1}$ and $D = 1.56\text{--}1.81 \text{ kpc}$ from Tomova & Tomov (1999), compositions of $\mu = 1.4$, $\gamma = 1$ and $Z = 1$ from Nussbaumer & Vogel (1987) and Spergel, Giuliani & Knapp (1983). These parameters yield a flux at 5 GHz of $S_c = 12\text{--}26 \mu\text{Jy}$.

In contrast to AG Dra, the three other sources either have a small secondary companion and therefore Roche lobe overflow would be providing the mass-transfer, or as in the case for V1974 Cyg, radio

² In this paper we use the convention that the WD is designated as the primary object and the companion, or donor, is designated as the secondary. Subscripts 1 and 2 are used in mass and radius relationships to distinguish between these two objects.

emission would have faded and dissipated from the time of the last outburst in 1992.

3.2 Evaporated secondary wind

In the previous section it was shown that only the AGB binary AG Dra would have a strong enough secondary wind to emit significant radio emission. However, if the WD is radiating sufficient soft X-rays then a corona will be formed around the secondary star, which causes a strong stellar wind to be evaporated (Basko & Sunyaev 1973). This type of interaction has been investigated in the context of the supersoft sources by van Teeseling & King (1998, hereafter vTK98) and they show that the mass loss rate in the secondary caused by irradiation is

$$\dot{M}_7 \approx -3\phi \frac{r_2}{a_9} (m_2 L_{30} \eta_s)^{1/2} M_\odot \text{ yr}^{-1}, \quad (3)$$

where ϕ is an irradiation efficiency factor, r_2 is the radius of the secondary in solar units, a_9 is orbital separation in units of 10^9 m, m_2 is the mass of the secondary in solar units, L_{30} is the irradiation luminosity in units of 10^{30} J s^{-1} ($\equiv 10^{37} \text{ erg s}^{-1}$), η_s is an ionization efficiency parameter and \dot{M}_7 is given in units of 10^{-7} . It is reasonable, therefore, to assume that since the supersoft sources produce soft X-rays during quiescence from their sustained nuclear burning, that the majority (if not all) of the supersoft sources have mass losses that are wind dominated.

To obtain an estimate for the mass loss from the secondary caused by irradiation from the WD, some assumptions concerning the geometry of the system need to be made. In equation (3), the variable ϕ is an efficiency parameter representing the fraction of the face of the companion that is being radiated and the fraction of the wind mass escaping the system. Commentary on the importance of ϕ is given in Knigge, King & Patterson (2000), and a value of 1 is expected. The other unknown parameter in equation (3) is the efficiency of the incident radiation in driving a wind, η_s . For a wide range of temperatures, including the expected temperature of the irradiation (few 10^5 K), $\eta_s \approx 1$. We can

therefore calculate an estimation for the mass loss in the wind from the secondary, which is given in Table 2.

Together with the mass-loss rate and equation (1), the flux from the wind can be found. Unfortunately, the expected fluxes are not as precise as one would hope as a large number of important parameters such as composition (μ , γ and Z), wind temperature and velocity (T and v_∞) are unknown.

van Teeseling & King (1998) consider He II to be the main absorber of the WD radiation, which has implications concerning the composition and temperature of the resulting wind. The temperature of the wind will range from the ionization temperature of He II to the temperature of the incident radiation, so we use a wind temperature of $T \approx 5 \times 10^5$ in this paper. The composition of a purely He II wind would give values for the mean atomic weight ($\mu = 4$), the electron to ion number density ratio ($\gamma = 2$) and the ionic charge ($Z = 2$). It would be surprising if these were realistic values for the wind, but they are useful approximations and only enter the wind-flux equation (1) as $S \propto \mu^{-4/3} \gamma^{2/3} Z^{4/3}$ and so, small changes would not have a large effect on the estimation. The final variable to estimate is the wind velocity, v_∞ . vTK98 approximate the velocity to be 0.3 times the isothermal speed of sound. For speed of sounds of the order of $\sim 100 \text{ km s}^{-1}$ this would give approximate wind velocities of $\sim 30 \text{ km s}^{-1}$. Using these approximations to the wind gives flux estimates at 5 GHz (S_C) and 8.3 GHz (S_X) shown in Table 2.

3.3 White dwarf wind

We have tried to estimate the radio flux from a white dwarf wind, but the uncertainties are too large to confidently quote numbers. Both Bondi–Hoyle and Roche lobe overflow accretion cannot be used reliably to predict the mass-transfer rate, and therefore the amount of excess material that the white dwarf can process is also undetermined.

3.4 Observational comments to wind emission

From our MERLIN and VLA observations we can provide the flux

Table 2. System parameters and radio fluxes for the supersoft sources.

	RX J0019		AG Dra	V1974 Cyg	T Pyx
Secondary	Fv	Mv	K III ^a	M5 v	Mv ^a
Period	15.8 h ^c		554 d ^d	1.95 h ^e	1.8 h ^f
m_1	0.75 ^g		0.4–0.6 ^d	0.9 ± 0.2 ^h	1.2 ⁱ
m_2	1.5 ^g	0.31–0.44 ^j	~ 1.5 ^d	0.23 ± 0.08 ⁱ	0.12 ^k
r_2	1.3	0.36–0.49	28–32 ^d	0.27 ± 0.08	0.17 ^l
L_{30}	0.3–0.9 ^m		0.14 ⁿ	2 ^o	0.2 ^p
a_9	2.9	1.79–1.87	249	0.57 ± 0.04	0.57
M_7	1.3	0.18–0.52	0.17	1.0 ± 0.5	0.14
D (kpc)	2.1 ^m		1.7 ± 0.1 ^a	1.8 ^q	3.5 ± 1.0 ^r
T	5×10^{5r}		5×10^{5r}	5×10^{5r}	5×10^{5r}
$v_{\text{km s}^{-1}}$	60		60	60	60
R_C (R_\odot)	510	140–280	130	430 ± 150	120
R_X (R_\odot)	360	95–190	90	300 ± 110	80
S_C (theoretical secondary) (μJy)			12–26		
S_C (theoretical evaporated) (μJy)	110	7.5–31	11	110 ± 70	2.6 ± 1.4
S_X (theoretical evaporated) (μJy)	140	10–43	15	160 ± 100	3.5 ± 1.9
S_C (observed) (μJy)	<100		~ 1000	<120	<110
S_X (observed) (μJy)	<80		–	<100	<95

^aTomov, Tomova & Ivanova (2000). ^bSzkody & Feinswog (1988). ^cWill & Barwig (1996). ^dMikołajewska et al. (1995). ^eSkillman et al. (1997). ^fSchaefer et al. (1992). ^gMeyer-Hofmeister, Schandl & Meyer (1997). ^hRetter, Leibowitz & Ofek (1997). ⁱContini & Prialnik (1997). ^jDeufel et al. (1999). ^kClemens et al. (1998); Patterson (1998). ^lPaczyński (1971). ^mBeuermann et al. (1995). ⁿGreiner (2000). ^oKahabka & van den Heuvel (1997). ^pPatterson et al. (1998). ^qChochol et al. (1993); Rosino et al. (1996). ^rvan Teeseling & King (1998).

for AG Draconis and upper limits to the fluxes of the other three supersoft sources in this paper (presented in Table 2). Given the spread in the observable system parameters, the expected flux for all three non-detected sources is at, or below the 5σ cut-off for detection. The surprise in this analysis is with AG Dra where we detect with MERLIN two unresolved point sources with a combined flux of ~ 1 mJy. This is much larger than both the wind flux and an evaporated wind at that frequency of around $10\text{--}20$ μ Jy and so we can conclude either that the assumptions used in these models are unrealistic, or a different emission mechanism is producing the observed radio flux.

It could be significant that the only detected fluxes originate from a K giant secondary rather than F or M dwarfs. The geometry and accretion in AG Dra is not expected to be from Roche lobe overflow, but rather from the wind of the AGB secondary.

4 CONCLUSIONS

We have searched for quiescent, persistent radio emission from the northern hemisphere supersoft X-ray sources, and have taken a high-resolution image of the one known source with emission.

We have improved the radio positions, source size and flux from the persistent emitter AG Dra with MERLIN. The core is resolved at the milliarcsec scale into two components with a combined flux of ~ 1000 μ Jy. It is possible that the core detected in the VLA image has significant nebulosity and is resolved out by the higher MERLIN resolution. A possible southern component detected by the VLA was unconfirmed, although this could be caused by it having a flux that was lower than the noise in the MERLIN image, or also being resolved out.

No new emission was detected from RX J0019.8+2156, T Pyx and V1974 Cygni down to a 1σ rms noise level of around 20 μ Jy beam $^{-1}$. No emission was detected from any previously known Galactic or extragalactic source in the three, 104 arcsec 2 fields imaged, and we place upper limits on the radio emission from these sources.

We have investigated possible causes of radio emission from a wind environment, both directly from the secondary star, and also as a consequence, of the high X-ray luminosity from the WD.

A total of 17 new point sources were imaged with fluxes of between 100 and 1500 μ Jy giving an estimate to the density of sources with a flux >100 μ Jy of 200 deg $^{-2}$, at 5 GHz, in this region of the sky.

ACKNOWLEDGMENTS

RNO wishes to thank the hospitality of the MERLIN national facility at the Jodrell Bank Observatory, especially Tom Muxlow. SC acknowledges support from grant F/00-180/A from the Leverhulme Trust.

The National Radio Astronomy Observatory is a facility of the National Science Foundation operated under cooperative agreement by Associated Universities, Inc. MERLIN is a national facility operated by the University of Manchester on behalf of PPARC. This research has made use of the SIMBAD data base, operated at CDS, Strasbourg, France.

REFERENCES

Basko M. M., Sunyaev R. A., 1973, *ApSS*, 23, 117
 Becker C. M., Remillard R. A., Rappaport S. A., McClintock J. E., 1998, *ApJ*, 506, 880

Beuermann K. et al., 1995, *A&A*, 294, L1
 Bridle A. H., Schwab F. R., 1989, *ASP Conf. Series*, Vol. 6, Wide-field imaging I: Bandwidth and time-average smearing, Lecture 13 in *Synthesis Imaging in Radio Astronomy*. Astron. Soc. Pac., San Francisco, p. 247
 Chochol D., Hric L., Urban Z., Koszík R., Grygar J., Papousek J., 1993, *A&A*, 277, 103
 Clemens J. C., Reid I. N., Gizis J. E., O'Brien M. S., 1998, *ApJ*, 496, 352
 Continini M., Prialnik D., 1997, *ApJ*, 475, 803
 Cowley A. P., Schmidtke P. C., Hutchings J. B., Crampton D., McGrath T. K., 1993, *ApJ*, 418, L63
 Deufel B., Barwig H., Šimić D., Wolf S., Drory N., 1999, *A&A*, 343, 455
 Duerbeck W. H., Sitter W. C., 1987, *Ap&SS*, 131, 467
 Eyres S. P., Davis R. J., Bode M. P., 1996, *MNRAS*, 279, 249
 Fender R. P., Southwell K., Tzioumis A. K., 1998, *MNRAS*, 298, 692
 Greiner J., 2000, *New Astron.*, 5, 137
 Hjellming R. M., 1992, *IAUC* 5502
 Kahabka P., van den Heuvel E. P. J., 1997, *ARA&A*, 35, 69
 Knigge Ch., King A. R., Patterson J., 2000, *A&A*, 364, L75
 Leavitt H., 1914, *Astron. Nachr.*, 197, 407
 Leitherer C., Robert C., 1991, *ApJ*, 377, 629
 Margon B., Deutsch E. W., 1998, *ApJ*, 498, L61
 Meyer-Hofmeister E., Schandl S., Meyer F., 1997, *A&A*, 321, 245
 Mikołajewska J., Kenyon S. J., Mikołajewski M., Garcia M. R., 1995, *AJ*, 109, 1289
 Motch C., 1998, *A&A*, 338, L13
 Muxlow T. W. B., Wilkinson P. N., Richards A. M. S., Kellermann K. I., Richards E. A., Garrett M. A., 1999, *New AR*, 43, 623
 Nussbaumer H., Vogel M., 1987, *A&A*, 182, 51
 O'Brien T. J., Cohen J. G., 1998, *ApJ*, 498, L59
 Paczyński B., 1971, *ARA&A*, 9, 183
 Pakull M. W., Moch C., Bianchi L., Thomas H.-C., Guibert J., Beaulieu J. P., Grison P., Schaeidt S., 1993, *A&A*, 278, L39
 Patterson J., 1998, *PASP*, 110, 1132
 Patterson J. et al., 1998, *PASP*, 110, 380
 Quintrell H., Fender R. P., 1998, *A&A*, 335, 17
 Retter A., Leibowitz E. M., Ofek E. O., 1997, *MNRAS*, 286, 745
 Rosino L., Iijima T., Rafanelli P., Radovich M., Esenoglu H., Della Vale M., 1996, *A&A*, 315, 463
 Schaefer B. E., Landolt A. U., Vogt N., Buckley D., Warner B., Walker A. R., Bond H. E., 1992, *ApJS*, 81, 321
 Schaeidt S., Hasinger G., Trümper J., 1993, *A&A*, 270, L9
 Seaquist E. R., Kroqulec M., Taylor A. R., 1993, *ApJ*, 410, 260
 Shahbaz T., Livio M., Southwell K. A., Charles P. A., 1997, *ApJ*, 484, L39
 Shara M. M., Zurek D. R., Williams R. E., Prialnik D., Gilmozzi R., Moffat A. F. J., 1997, *AJ*, 114, 258
 Skillman D. R., Harvey D., Patterson J., Vanmunster T., 1997, *PASP*, 109, 114
 Southwell K. A., Livio M., Charles P. A., O'Donoghue D., Sutherland W. J., 1996, *ApJ*, 470, 1065
 Spergel D. N., Giuliani J. L., Jr, Knapp G. R., 1983, *ApJ*, 275, 330
 Szkody P., Feinswog L., 1988, *ApJ*, 334, 422
 Tomov T., Munari U., Kolev D., Tomasella L., Rejkuba M., 1998, *A&A*, 333, L67
 Tomov N. A., Tomova M. T., 1999, *A&A*, 347, 151
 Tomov N. A., Tomova M. T., Ivanova A., 2000, *A&A*, 364, 557
 Torbett M. V., Campbell B., 1987, *ApJ*, 318, L29
 van den Heuvel E. P. J., Battacharya D., Nomoto K., Rappaport S., 1992, *A&A*, 262, 97
 van Teeseling A., King A. R., 1998, *A&A*, 338, 957 (vTK98)
 Will T., Barwig H., 1996, in Greiner J., ed., *Workshop on Supersoft X-ray sources*, Garching, Lecture Notes in Physics No 472. Springer-Verlag, Berlin, p. 99
 Williams R. E., 1982, *ApJ*, 261, 170
 Wright A. E., Barlow M. J., 1975, *MNRAS*, 170, 41

This paper has been typeset from a $\text{\TeX}/\text{\LaTeX}$ file prepared by the author.